Analytical Letters

ISSN: (Print) (Online) Journal homepage: https://www.tandfonline.com/loi/lanl20

Determination of Rhodamine B in Cosmetics, Candy, Water, and Plastic by a Novel Multiwalled Carbon Nanotube (MWCNT)@Zinc Oxide@Magnetite Nanocomposite for Magnetic Solid-Phase Extraction (MSPE) with Spectrophotometric Detection

Nebiye Kizil, Duygu Erbilgin, Erkan Basaran, Mehmet Lütfi Yola, Erkan Yilmaz, Salsabil Marouch & Mustafa Soylak

To cite this article: Nebiye Kizil, Duygu Erbilgin, Erkan Basaran, Mehmet Lütfi Yola, Erkan Yilmaz, Salsabil Marouch & Mustafa Soylak (2023): Determination of Rhodamine B in Cosmetics, Candy, Water, and Plastic by a Novel Multiwalled Carbon Nanotube (MWCNT)@Zinc Oxide@Magnetite Nanocomposite for Magnetic Solid-Phase Extraction (MSPE) with Spectrophotometric Detection, Analytical Letters, DOI: 10.1080/00032719.2023.2243353

To link to this article: https://doi.org/10.1080/00032719.2023.2243353

Published online: 07 Aug 2023.

ANALYTICAL LETTERS
https://doi.org/10.1080/00032719.2023.2243353

Taylor & Francis
Taylor & Francis Group

SAMPLE PREPARATION

Determination of Rhodamine B in Cosmetics, Candy, Water, and Plastic by a Novel Multiwalled Carbon Nanotube (MWCNT)@Zinc Oxide@Magnetite Nanocomposite for Magnetic Solid-Phase Extraction (MSPE) with Spectrophotometric Detection

Nebiye Kizil[a,b], Duygu Erbilgin[b], Erkan Basaran[b], Mehmet Lütfi Yola[c], Erkan Yilmaz[d,e], Salsabil Marouch[e,f], and Mustafa Soylak[g,h,i]

[a]Department of Basic Sciences, Faculty of Engineering, Hasan Kalyoncu University, Gaziantep, Turkey; [b]Environmental Research and Application Center, Hasan Kalyoncu University, Gaziantep, Turkey; [c]Department of Nutrition and Dietetics, Faculty of Health Sciences, Hasan Kalyoncu University, Gaziantep, Turkey; [d]Department of Analytical Chemistry, Faculty of Pharmacy, Erciyes University, Kayseri, Turkey; [e]Nanotechnology Research Center (ERNAM), Erciyes University, Kayseri, Turkey; [f]Laboratory of Chemistry and Environmental Chemistry (LCCE), Department of Chemistry, Faculty of Matter Sciences, Batna-1 University, Batna, Algeria; [g]Department of Chemistry, Science Faculty, Erciyes University, Kayseri, Turkey; [h]Technology Research and Application Center (TAUM), Erciyes University, Kayseri, Turkey; [i]Turkish Academy of Sciences (TUBA), Cankaya, Turkiye

ABSTRACT

A new magnetic solid phase microextraction method (MSPE) was developed for the preconcentration of rhodamine B from plastics, cosmetics, and environmental samples before spectrophotometric analysis. A nanocomposite adsorbent containing ZnO nanoparticles (NPs), multi-walled carbon nanotubes (MWCNTs) and Fe_3O_4 nanoparticles was synthesized by a hydrothermal procedure. The new magnetic nanocomposite (MWCNTs@ZnO@Fe_3O_4) was characterized by Fourier-transform infrared spectroscopy (FT-IR), x-ray diffraction (XRD), and scanning electron microscopy (SEM). The pH, sample volume, eluent type, adsorbent mass, influence of foreign species, and analyte-adsorbent and eluent contact times were optimized. The optimum pH was 3; adsorbent mass, 20 mg; sample volume, 50 mL; and eluent, 0.7 mL of ethanol. Recovery values exceeding 95% were obtained. The developed vortex assisted magnetic solid phase extraction method (VA-MSPE) was applied to practical analysis. The limits of detection (LOD) and quantification (LOQ) were 0.83 μg L^{-1} and 2.77 μg L^{-1}, respectively. The addition/recovery experiments were carried on several water samples to demonstrate acceptable recoveries.

ARTICLE HISTORY
Received 28 April 2023
Accepted 28 July 2023

KEYWORDS
Magnetic solid phase extraction; multiwalled carbon nanotubes; rhodamine B; spectrophotometry

CONTACT Mustafa Soylak soylak@erciyes.edu.tr Department of Chemistry, Science Faculty, Erciyes University, Kayseri 38039, Turkey; Turkish Academy of Sciences (TUBA), Bayraktar Mahallesi, Vedat Dalokay Caddesi No: 112, 06670 Cankaya, Ankara, Turkey.

Introduction

Synthetic and natural dyes are increasingly used in rubber, textiles, food, papermaking, leather, plastic, and cosmetics (Hayeeye et al. 2017). The dyes are generally stable against heat, light and oxidizing agents. In addition, they are often difficult to biodegrade. Because of the increasing production, the formation of wastewater is also increasing, especially in the textile industry. These dyes contained in wastewater, mix with environmental water samples, and change the color of the water, prevent the passage of sunlight and reduce the biological diversity (Ozkantar, Soylak and Tuzen 2017; Wang et al. 2006).

Rhodamine B, which is reddish violet in water, is a red xanthene dye (triphenylmethane dyes) and its trade name is D&C Red No. 19. It is one of the most employed industrial-based dyes due to its low cost, and is also employed as a tracer and fluorescent colorant (Anirudhan, and Ramachandran 2015; Jain et al. 2007; Richardson, Wilson, and Rusch 2004).

It is present the environmental water because of its utility in many industrial applications. This situation poses a danger to the health of humans and all living things due to the dangerous effects of rhodamine B. It causes unhealthy effects for aquatic creatures and negative effects such as respiratory toxicity, reproductive problems, chronic toxicity, neurotoxicity, carcinogenicity, and skin irritation (Best et al. 2010; Hasegawa et al. 2009; Hu et al. 2013; Jain et al. 2007; Kim et al. 2008; Li et al. 2011; Ozkantar, Soylak, and Tuzen 2017; Yuan, Lin, and Feng 2011; Zhang et al. 2009). Due to the harmful effects mentioned above, both separation and determination of rhodamine B in water, food, plastic products, and especially cosmetic products are mandatory (Bello et al., 2019; Cui et al. 2015; Ozkantar, Soylak, and Tuzen 2017; Ruthven 1984; Suzuki 1993). The treatment of wastewater including toxic dose synthetic or naturel dyes is one of the most vital procedures for the protection of the environment.

To this end, there are diverse techniques for its determination, such as bio-treatment, chemical oxidation, ion exchange, flotation, coagulation, electrochemical processes, photocatalysis, and adsorption (Jain et al. 2007). Among the many treatment methods, adsorption is a solid phase extraction method in which dyes and heavy metals are removed and determined in water (Hasegawa et al. 2009; Hayeeye et al. 2017; Kotsmar et al. 2010; Schieder et al. 1994). Adsorption is low cost, easy, and has practically applicable operation and reaction conditions providing the decrease of the formation of chemical waste. In addition, it is an increasingly popular with the use of different adsorbents, as it has high selectivity and practical designability. Adsorption is an important step in the solid phase extraction to separate the analyte from the sample. Therefore, in order to carry out the most effective adsorption process, it is necessary to employ an adsorbent with the best performance (Chen et al. 2022; Li et al. 2015; Tercan et al. 2023; Zhang, and Selim 2005).

Many adsorbents such as graphene oxide (GO) (Zhou et al. 2022), carbon nanotubes (CNTs) (Aydin, Cakmak, et al. 2020), polymeric materials (Soylak et al. 1997; Soylak and Yilmaz 2010), activated carbon (Ghaedi et al. 2016; Soylak and Maulana 2023), and ion exchange resins (Ma et al. 2023) are used because of their surface area, availability, cost, and performance. These carbon-containing materials are employed in chemistry, medicine, energy, and materials.

CNTs include single-walled carbon nanotubes (SWCNT) and multi-walled carbon nanotubes (MWCNT), classified by the number of concentric tubes. SWCNT has one layer of graphene cylindrical wall and MWCNT has two or more graphene shells which are concentric and cylindrical (Han et al. 2009; Ma et al. 2010; Zhang et al. 2023). In addition, CNTs have high electrical conductivity, large surface area, simple electron transfer, and good thermal stability. Hence, they offer an appropriate catalyst for dyes and metallic species (Kennedy et al. 2017; Tourchi Moghadam and Seifi 2022).

However, the low-dose use of CNTs in nanomaterials may notably improve mechanical properties and control the structure of the composite (Lee et al. 2010; Sldozian et al. 2019; Wang et al. 2022). Thus, CNTs are combined with semiconductor materials such as ZnO and MgO to improve the physical and mechanical properties. The ZnO/CNTs combination provides a large surface area for the CNTs and increases the conductivity (Kennedy et al. 2017; Kumar et al. 2015; Nodeh et al. 2016; Sun et al. 2019; Tourchi Moghadam and Seifi 2022; Xolani et al. 2017). Although CNTs/ZnO adsorption is reliable, it is time consuming and causes analyte losses. In order to improve the performance, CNTs have included Fe_3O_4 to provide magnetic properties (Azam and Mohammad 2015; Nodeh et al. 2015; 2016; Yadollah, Mohammad, and Mahnaz 2015).

In this paper, an MWCNTs@ZnO@Fe_3O_4 nanocomposite was synthesized by utilizing hydrothermal procedure to determine rhodamine B in plastic and cosmetics. The simple VA-MSPE method for the determination of rhodamine B reduces time and chemical consumption and offers high recoveries, suitable enrichment factors, and good efficiency.

Experimental

Instrumentation

Rhodamine B determination was performed with an ultraviolet-visible spectrophotometer from Perkin-Elmer (Lambda 25; Norwalk, CT, USA). A vortex mixer (Stuart SA8 BioCote, UK) was used to augment the extraction efficiency of rhodamine B. The pH of sample solutions was optimized by means of pH/ORP Meter (Hanna Hı 2211, USA). Distilled water was acquired from the Nuve Water Distiller ND-4 (Ankara, Turkey).

The surface functional groups such as Zn–O bond and C = C bond were characterized by Fourier transform infrared spectroscopy (FT-IR, Thermo Scientific Nicolet 6700) using attenuated total reflectance. A Zeiss Evo LS10 scanning electron microscope (SEM) was operated at 10 kV. The crystal structure of the materials was characterized using a Bruker AXS D8 x-ray powder diffractometer.

Reagents

Analytical grade MWCNTs (Nanography, Turkey), sodium dodecyl sulfate (SDS) (Carlo Erba, France), ammonium bicarbonate (NH_4HCO_3) (Sigma Aldrich, Germany), zinc chloride ($ZnCI_2$), iron (III) chloride ($FeCl_3.\ 6H_2O$), iron (II) chloride ($FeCl_2.4H_2O$), and ammonia (NH_3) (Merck, Germany) were used without purification in the synthesis of nanomaterials.

The rhodamine B stock solution (1.0×10^{-4} M) was prepared in analytical grade ethanol. The model solutions and standard solutions were prepared by diluting the rhodamine B stock solution in ethanol.

Optimization for pH values from 2.0 to 8.0 were carried out employing buffers such as ammonium, phosphate, and acetate. Analytical reagent grade ethanol with was used for the desorption of rhodamine B from MWCNTs@ZnO@Fe_3O_4.

Synthesis of mangnetic MWCNTs@ZnO@Fe_3O_4 nanomaterial

A hydrothermal technique was used for the synthesis of ZnO@MWCNTs. Solutions of $ZnCl_2$ (1.0 M, 15.0 mL) and NaOH (5.0 M, 25.0 mL) were mixed and the MWCNTs (0.25 g) were slowly added with stirring. The mixture was dispersed in an ultrasonic bath for 30 min, transferred into a Teflon-lined stainless steel hydrothermal unit, and heated to 180 °C for 12h. The obtained MWCNTs@ZnO nanomaterial was washed twice with deionized water and acetone, dried at 60 °C, and ground before use (Yang et al. 2008).

The synthesis of MWCNTs@ZnO@Fe_3O_4 nanomaterial was performed by a hydrothermal method using a reflux system under nitrogen. 100 g of MWCNTs@ZnO were dispersed in 100 mL of deionized water. 50 mL of water containing $FeCl_3$ (0.745 g) and $FeCl_2$ (0.340 g) were slowly introduced at 85 °C. After 1 h, 20.0 mL of NH_3 (25.0%) were added dropwise and allowed to react for 1 h. The mixture was cooled, filtered, washed twice with distilled water and acetone, and dried at 60 °C (Jiang et al. 2023; Li et al. 2023; Soylak, Acar, and Yilmaz 2017; Wang et al. 2023; Wu et al. 2022; Xu et al. 2022; 2023).

VA-MSPE

A model solution (10 mL; pH 3.0) was employed for the optimization of the VA-MSPE method. The model solution was treated with 20.0 mg of the MWCNTs@ZnO@Fe_3O_4 adsorbent. The model solution and MWCNTs@ZnO@Fe_3O_4 particles were vortex mixed for 3 min. The adsorbent was subsequently isolated from an aqueous solution by applying an external neodymium magnet. Lastly, the isolated MWCNTs@ZnO@Fe_3O_4 particles were subjected to desorption by adding 0.7 mL of ethanol to the remaining adsorbent vortex mixing to elute the rhodamine B from MWCNTs@ZnO@Fe_3O_4. The ethanol phase containing rhodamine B dye was analyzed by spectrophotometry at 558 nm. A similar VA-MSPE methodology was applied for blanks.

Analysis of cosmetics, water, and plastic

The developed VA-MSPE method was applied to cosmetics, water and plastic samples. The cosmetics including nail polish, lip balm and rose water obtained from a market in Gaziantep, Turkey.

About 5 mg nail polish, rouge or lip balm; 3 g cand; 1 g candle; 6 g ballon; and 1 g paper napkin were weighed into centrifuge tubes and dissolved in 5 mL ethanol with shaking for 1 hour to isolate rhodamine B. Environmental water samples were passed through a 0.22 μm filter before VA-MSPE application and stored at 4 °C. The samples were

centrifuged for 10 minutes before using the developed MSPE method upon the liquid phase. The absorbance measurements were carried out by spectrophotometry at 558 nm.

Results and discussion

Characterization of the adsorbent

The filamentous and smooth structure of MWCNTs and the small spherical particles of ZnO in the MWCNTs@ZnO nanomaterial are shown in Figure 1A. Figure 1B shows the nanomaterial's morphological structure. The Fe_3O_4 nanospheres of various sizes form a layer on the top of MWCNTs@ZnO.

Figure 2A shows the XRD pattern of the synthesized nanomaterials. The MWCNTs@ZnO have diffraction peaks from both MWCNTs and ZnO NPs. The characteristic peaks and the corresponding latices of ZnO NPs are located at $2\theta = 31.76°$ (100), 34.4° (002), 36.2° (101), 47.57° (102), 56.55° (110), 62.86° (103), 66.4° (200), 67.9° (112), and 69.10° (201). According to these peaks, the structure of the formed ZnO NPs is wurtzite single phase with a hexagonal unit. The MWCNTs provided a peak at $2\theta = 26.8°$ due to the (002) reflection of graphite for the nanomaterial. Characteristic peaks at 30.37 (220), 36.07° (311), 42.09° (400), 56.74 (511), and 62.8 (440) were observed due to the cubic phase of Fe_3O_4 (Elhamdi et al. 2022; Ramoraswi, and Ndungu 2015; Yang et al. 2018).

The infrared spectra of the synthesized materials are shown in Figure 2B. The spectra affirm the presence of ZnO NPs and MWCNTs. The MWCNTs@ZnO showed a significant vibration at 540 cm^{-1} corresponding to the characteristic stretching of Zn–O and a band at 1535 cm^{-1} due to the C = C bond of MWCNTs. The MWCNTs@ZnO@Fe_3O_4 spectrum showed the same band corresponding to Zn–O vibration. However, the band was a larger due to the overlapping vibration of the Fe–O bond at 551 cm^{-1} (Anžlovar et al. 2012; Jannah and Onggo 2019).

Influence of pH

The pH optimization is one of the most important parameters affecting adsorption because it determines the charge balance of the medium (Hema and Arivoli 2009; Rais and Rajeev 2010; Ramuthai et al. 2009). The sample pH was controlled using buffer

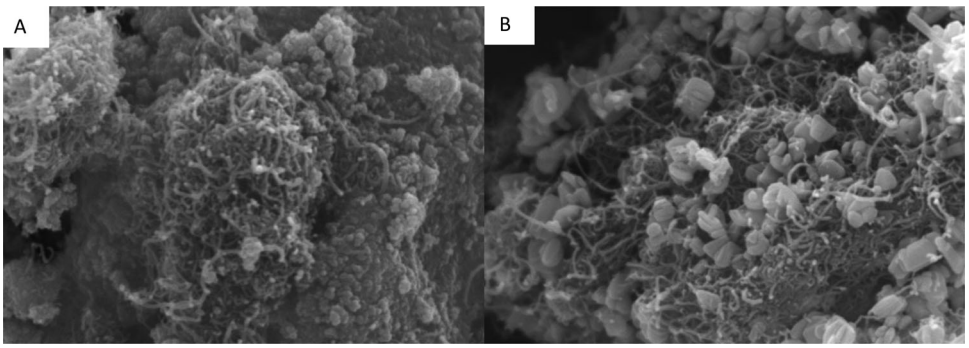

Figure 1. FE-SEM images of (A) MWCNTs@ZnO and (B) MWCNTs@ZnO@Fe_3O_4.

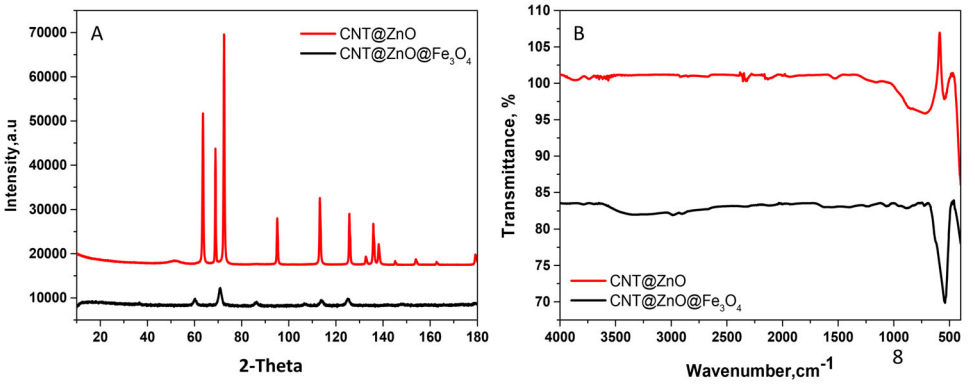

Figure 2. (A) X-ray diffraction patterns and (B) infrared spectra of MWCNTs@ZnO and MWCNTs @ZnO@Fe_3O_4.

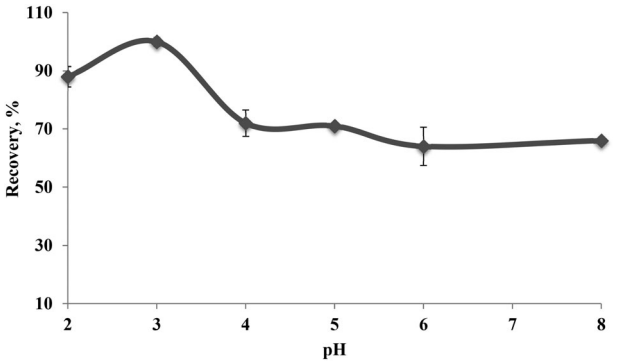

Figure 3. Influence of pH upon the extraction efficiency of rhodamine B by MWCNTs@ZnO@Fe_3O_4 ($n = 3$) Conditions: eluent volume: 0.7 mL, adsorbent dosage: 20.0 mg.

solutions from pH 2.0 to 8.0. The recovery values for rhodamine B are shown in Figure 3. The optimum pH was 3.0 where the maximum recovery was obtained.

Mass of MWCNTs@ZnO@Fe_3O_4

The mass of MWCNTs@ZnO@Fe_3O_4 NPs was investigated from 5.0 to 40.0 mg using VA-MSPE with spectrophotometric detection. The recoveries of rhodamine B increased up to 10.0 mg (Figure 4) and reached a plateau. In order to ensure sufficient adsorbent, 20.0 mg of MWCNTs@ZnO@Fe_3O_4 NPs were deemed to be optimum and were used in subsequent measurements (Khan, Dahiya, and Ali 2012; Namasivayam et al. 2019).

Influence of eluent type and volume

Complete desorption of rhodamine B from MWCNTs@ZnO@Fe_3O_4 NPs is necessary to obtain quantitative extraction by VA-MSPE. Therefore, the desorption solvent must elute the analyte with high recoveries. Acetonitrile, ethanol, acetone, and water were

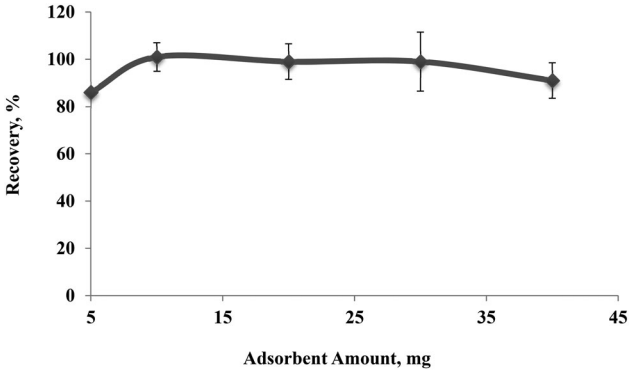

Figure 4. Influence of the MWCNTs@ZnO@Fe_3O_4 NPs mass upon the extraction efficiency of rhodamine B ($n = 3$). Conditions: pH: 3, eluent volume: 0.7 mL.

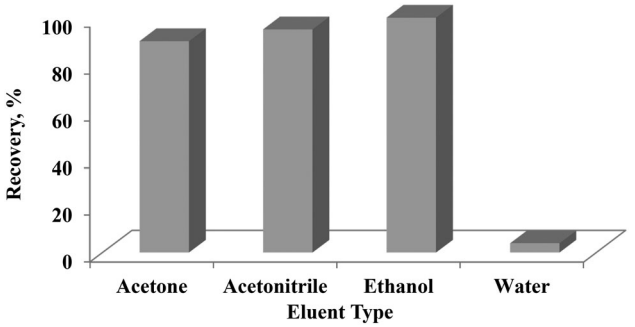

Figure 5. Influence of the eluent type upon the extraction efficiency of rhodamine B ($n = 3$). Conditions: pH: 3.0, eluent volume: 0.7 mL, adsorbent dosage: 20.0 mg.

investigated in this study. Although quantitative recoveries were obtained with acetonitrile, ethanol and acetone, ethanol was selected for further work (Figure 5).

Next, the lowest eluent volume that provided quantitative elution of rhodamine B was investigated to minimize its volume and provide a high preconcentration factor. Thus, desorption experiments were carried out from 0.7 to 3.0 mL with spectrophotometric analysis. The results show that 0.7 mL of ethanol were sufficient to quantitatively elute rhodamine B from 20.0 mg MWCNTs@ZnO@Fe_3O_4 NPs.

Contact time of adsorbate and analyte

In extraction procedures, vortex mixers, mechanical shakers and ultrsound are used to increase the interaction between the analyte with the adsorbent and eluent. In this study, vortex mixing was used in both adsorption and desorption processes to achieve simple and fast extraction. The model solutions were vortex mixed from 2 to 7 minutes to optimize the contact time between MWCNTs@ZnO@Fe_3O_4 NPs and rhodamine B. Quantitative recovery values were obtained with vortex shaking for 3 minutes as shown in Figure 6.

The desorption period for vortex mixing was also optimized by varying the interaction time of ethanol and MWCNTs@ZnO@Fe_3O_4 NPs from 2 to 10 min. The results

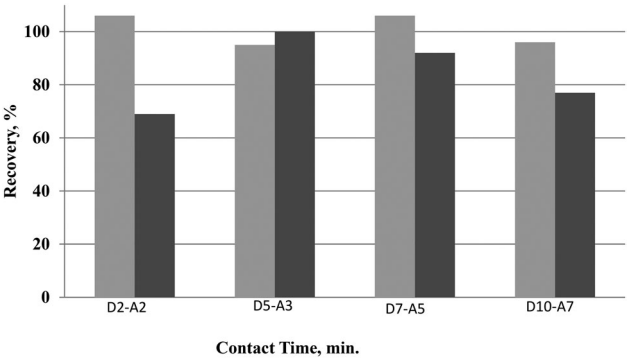

Figure 6. Influence of vortex mixing time upon the adsorption and desorpsiton efficiency of rhodamine B on MWCNTs@ZnO@Fe_3O_4 where D is desorption and A is adsorption ($n = 3$) Conditions: pH: 3.0, eluent volume: 0.7 mL, adsorbent dosage: 20.0 mg.

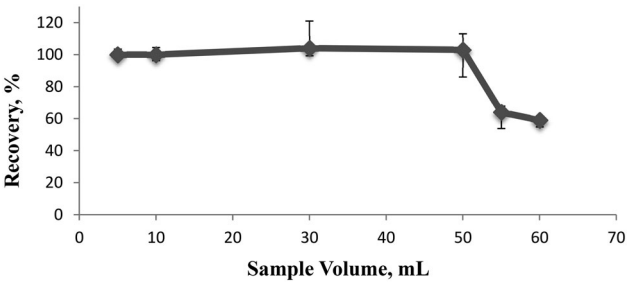

Figure 7. Influence of the sample volume upon the isolation of rhodamine B ($n = 3$). Conditions: pH: 3.0, eluent volume: 0.7 mL, adsorbent dosage: 20.0 mg.

in Figure 6 show that a desorption period of 2 min is sufficient to quantitatively elute rhodamine B from the adsorbent. Hence, the adsorption and desorption of rhodamine B by VA-MSPME were rapid and efficient.

Influence of sample volume

Finding the highest sample volume to which the separation/enrichment-based methods is significant to obtain a low detection limit, achieving high enrichment, and reducing matrix interference. Herein, the developed VA-MSPME method was applied to model solutions with volumes from 5.0 to 60.0 mL. The recoveries for rhodamine B were over 95.0% up to 50.0 mL (Figure 7). Quantitative recoveries were not obtained at 55.0 mL and 60.0 mL. The obtained results show that the developed VA-MSPE method may be applied to 50.0 mL sample volumes. Since the final volume was 0.7 mL, the preconcentration factor was determined to be 71.4.

Matrix effects

For separation/enrichment methods, the ability to selectively isolate the analyte from the matrix and accurately determine it without interferences is necessary (Aydin,

Table 1. Influence of foreign species as mean ± standard deviation upon the extraction efficiency of the VA-MSPE spectrophotometric procedure ($n = 3$).

Foreign species	Concentration, mg L^{-1}	Recovery, %
Chromotrope FB	5	100 ± 7[a]
RBV-5	2.2	94 ± 8
Methylene blue	1.6	95 ± 8
Lissamine green B	1.73	103 ± 3
Eosin B	0.58	94 ± 2
Sudan IV	1.14	99 ± 13
Mn^{2+}	100	102 ± 2
Al^{+3}	100	101 ± 5
Cd^{2+}	100	100 ± 1
Cu^{2+}	10	99 ± 3
Co^{2+}	100	96 ± 4
Na^{+}	5000	99 ± 1
Mo^{2+}	5	98 ± 6

Conditions: pH: 3, eluent volume: 0.7 mL, adsorbent dosage: 20 mg, rhodamine B concentration: 2.0×10^{-6} M.
[a]Mean ± standard deviations.

Yilmaz, et al. 2020; Gokce et al. 2023; Sotouneh et al. 2023; Soylak 1998). Several potential interferences at different concentrations were investigated with VA-MSPE. Potential interferents included Sudan IV, chromotrope FB, RBV-5R, metilen blue, eosin B, lissamine green B, Chicago sky blue, Al^{3+}, Cd^{2+}, Mo^{2+}, Co^{2+}, and Na^{+}. The tolerance was deemed to be the concentration of matrix species that induced a relative error of 5% in the determination of rhodamine B. The analyte was affected by different concentrations of the interferents as shown in Table 1. In general, the results show that the VA-MSPE provided good selectivity (Altunay et al. 2022).

Real samples applications

The accuracy of VA-MSPE method was investigated by the analysis of cosmetics and plastic. The addition/recovery experiments were used to determine the accuracy of VA-MSPE using tap water under the optimum conditions. The recovery values between 83% and 97% (Table 2) demonstrate that the developed VA-MSPE provided good accuracy for the determination of rhodamine B in cosmetics, water, and plastic (Table 3).

Analytical performance

In order to validate the VA-MSPME method, the relative standard deviation (RSD), preconcentration factor (PF), limit of quantification (LOQ), correlation coefficient (R^2), limit of detection (LOD), and linear range (LR) were evaluated under the optimum conditions. The relative standard deviation was 3.8%. The correlation coefficient, limit of detection ($3S_b/m$), and limit of quantification ($10S_b/m$) were 0.9941, 0.83 μg L^{-1}, and 2.77 μg·L^{-1} from the calibration relationship where m is the slope and S_b is the standard deviation. The linear calibration relationship was $A = 0.1423C + 0.0114$ where A is the absorbance and C is the rhodamine B concentration. The preconcentration factor for rhodamine B was 71.4.

Table 2. Addition/recovery experiments of rhodamine B as mean ± standard deviation in tap water using the VA-MSPE spectrophotometric procedure ($n = 3$).

Added ($\mu g \cdot L^{-1}$)	Measured ($\mu g \cdot L^{-1}$)	Recovery, %
0.0	Not detected	–
3.41	3.29 ± 0.15	96 ± 4
6.84	6.57 ± 0.05	97 ± 1
13.69	11.38 ± 0.49	83 ± 1

Conditions: pH: 3.0, eluent volume: 0.7 mL, adsorbent dosage: 20.0 mg.

Table 3. Determination of rhodamine B as mean ± standard deviation using the VA-MSPE spectrophotometric procedure ($n = 3$).

Samples	Measured
Dragee candy	3.96 ± 0.04 μg/g[a]
Cake decoration sugar	4.55 ± 0.27 μg/g
Party candle	44.6 ± 3.7 μg/g
Nail polish 1	72.5 ± 8.3 μg/g
Rouge 1	36.5 ± 5.6 μg/g
Plastic balloon	7.1 ± 0.2 μg/g
Rose water	Below the limit of detection
Nail polish remover	0.17 ± 0.04 μg/mL
Paper napkin	84 ± 4 μg/g

Conditions: pH: 3.0, eluent volume: 0.7 mL, adsorbent dosage: 20.0 mg.
[a]Mean ± standard deviations.

Table 4. Comparison between the developed procedure with the literature.

Method	Limit of detection	Relative standard deviation, %	Enhancement factor	Reference
Solid phase extraction	0.52 $\mu g\ L^{-1}$	–	125	Beyki, Feizi, and Shemirani 2016
Ionic liquid-based dispersive liquid–liquid Microextraction (IL-based DLLME)	1.05 $\mu g\ L^{-1}$	1.3	65	Taziki et al. 2012
Solid phase extraction	0.22 $\mu g\ L^{-1}$	4.8	140	Bisgin et al. 2020
Solid-phase extraction	3.6 $\mu g\ L^{-1}$	3.83–6.019		Wu et al. 2015
Dispersive liquid–liquid microextraction	2.39 ng mL^{-1}	2.88	10	Biparva, Ranjbari, and Hadjmohammadi 2010
Solid-phase extraction	3.4 $\mu g\ L^{-1}$	–	–	Su et al. 2015
Solid-phase extraction	3.94 $\mu g\ L^{-1}$	1.16	26	Nekoeinia et al. 2015
Solid-phase extraction	5.2 ng mL^{-1}	3.1		Bakheet and Zhu 2017
Magnetic solid-phase extraction	0.83 $\mu g\ L^{-1}$	3.8	71.4	This work

Conclusions

The goal of this work is to demonstrate that the separation and preconcentration of rhomamine B from cosmetics and plastics is within the scope of green chemistry. Each of the samples was analyzed by VA-MSPME as described above. The aqueous solutions were analyzed by spectrophotometry for rhodamine B. The isolation conditions were optimized. As a result, 20 mg of adsorbent, 3 minutes adsorption time, 2 minutes

desorption time, and 0.7 mL desorption solvent were optimum to separate and preconcentrate rhodamine B. The optimum recovery was obtained at pH 3.

The method was applied directly to the analysis of cosmetics and plastics. The accuracy was verified by recovery experiments as shown in Table 1. The microextraction method demonstrated offers rapid analysis, low chemical consumption, easy magnetic separation, high recoveries, good extraction efficiency, and a suitable preconcentration factor (PF). However, the protocol has some minor disadvantages. For example, it is not applicable across a wide pH range.

The developed VA-MSPME was compared with the literature as shown in Table 4. This approach is superior to previous methods for rhodamine B because of the low limit of detection and high preconcentration factor without external treatment.

Disclosure statement

No potential conflict of interest was reported by the author(s).

ORCID

Nebiye Kizil http://orcid.org/0000-0003-4994-1680

References

Altunay, N., M. Tuzen, B. Hazer and A. Elik. 2022. Synthesized of a novel xanthate functionalized polypropylene as adsorbent for dispersive solid phase microextraction of caffeine using orbital shaker in mixed beverage matrices. *Food Chemistry* 393:133464. doi:10.1016/j.foodchem.2022.133464.

Anirudhan, T. S., and M., Ramachandran. 2015. Adsorptive removal of basic dyes from aqueous solutions by surfactant modified bentonite clay (organoclay): kinetic and competitive adsorption isotherm. *Process Safety and Environmental Protection* 95:215–225. doi:10.1016/j.psep.2015.03.003.

Anžlovar, A., Z. Crnjak Orel, K. Kogej and M. Žigon. 2012. Polyol-mediated synthesis of zinc oxide nanorods and nanocomposites with poly (methyl methacrylate). *Journal of Nanomaterials* 31: 760872. doi:10.1155/2012/760872.

Aydin, F., R. Cakmak, A. Levent, and M. Soylak, 2020. Silica gel-immobilized 5-aminoisophthalohydrazide: a novel sorbent for solid phase extraction of Cu, Zn and Pb from natural water samples. *Applied Organometallic Chemistry* 34: e5481 doi:10.1002/aoc.5481.

Aydin, F., Yilmaz, E., Ölmez, E., and M. Soylak, 2020. Cu_2O-CuO ball like/multiwalled carbon nanotube hybrid for fast and effective ultrasound-assisted solid phase extraction of uranium at ultra-trace level prior to ICP-MS detection. *Talanta*, 207: 120295. doi:10.1016/j.talanta.2019.120295.

Azam, S. and A., Mohammad. 2015. Magnetic Fe_3O_4@C nanoparticles modified with 1-(2-thiazolylazo)-2-naphthol as a novel solid-phase extraction sorbent for preconcentration of copper (II). *Microchimica Acta* 182: 257–264. doi:10.1007/s00604-014-1327-1.

Bakheet, A. A. A., and X. S., Zhu. 2017. Determination of rhodamine B in food samples by Fe_3O_4@ionic liquidsβ-cyclodextrin cross linked polymer solid phase extraction coupled with fluorescence spectrophotometry. *Journal of Fluorescence* 27: 1087–1094. doi:10.1007/s10895-017-2042-1.

Bello, O. S., K. A., Adegoke, S. O., Fagbenro, and O. S., Lameed. 2019. Functionalized coconut husks for rhodamine-B dye sequestration. *Applied Water Science* 9:189. doi:10.1007/s13201-019-1051-4.

Best, A. Q., R. Xu, M. E. McCarroll, L. Wang, and D. J. Dyer. 2010. Design and investigation of a series of rhodamine-based fluorescent probes for optical measurement of pH. *Organic Letters*. 12:3219–3221. doi:10.1021/ol1011967.

Beyki, M. H., F. Feizi, and F. Shemirani. 2016. Melamine-based dendronized magnetic polymer in the adsorption of Pb(II) and preconcentration of rhodamine B. *Reactive and Functional Polymers*. 103:81–91. doi:10.1016/j.reactfunctpolym.2016.04.006.

Biparva, P., E. Ranjbari, and M. R. Hadjmohammadi. 2010. Application of dispersive liquid–liquid microextraction and spectrophotometric detection to the rapid determination of rhodamine 6G in industrial effluents. *Analytical Chimica Acta* 674:206–210. doi:10.1016/j.aca.2010.06.024.

Bisgin, A. T., Y. Sürme, M. Uçan, and M. Narin. 2020. Simultaneous preconcentration and determination of rhodamine B and brilliant blue. *Iranian Journal of Science and Technology*. 44: 695–705. doi:10.1007/s40995-020-00892-6.

Chen, X., K. Hu, J. Zhou, X. Yuan, M. Zhang, K. Huang and Y. Pan 2022. Critical evaluation of the application of filter-assisted separation in analytical atomic spectrometry. *Applied Spectroscopy Reviews, in press*. doi:10.1080/05704928.2022.2134145.

Cui, L., Y. Wang, L. Gao, L. Hu, L. Yan, Q. Wei, and B. Du. 2015. EDTA functionalized magnetic graphene oxide for removal of Pb(II), Hg(II) and Cu(II) in water treatment: Adsorption mechanism and separation property. *Chemical Engineering Journal* 281:1–10. doi:10.1016/j.cej.2015.06.043.

Elhamdi, I., H. Souissi, O. Taktak, J. Elghoul, S. Kammoun, E. Dhahri, and B. F. O. Costa. 2022. Experimental and modeling study of ZnO:Ni nanoparticles for near-infrared light emitting diodes. *RSC Advances*. 12 (21):13074–13086. doi:10.1039/d2ra00452f.

Ghaedi, M., F. N. Azad, K. Dashtian, S. Hajati, A. Goudarzi, and M. Soylak, 2016. Central composite design and genetic algorithm applied for the optimization of ultrasonic-assisted removal of malachite green by ZnO nanorod-loaded activated carbon. *Spectrochimica Acta Part A: Molecular and Biomolecular Spectroscopy* 167: 157–164. doi:10.1016/j.saa.2016.05.025.

Gokce, S., A. Hol and E. Ersin 2023. Determination of cobalt (II), copper (II), lead (II), and zinc (II) with preconcentration by 8-hydroxyquinoline-coated magnetic nanoparticles (MNPs) and microinjection sampling–flame atomic absorption spectrometry (MIS–FAAS). *Analytical Letters* 56: 1784–1802. doi:10.1080/00032719.2022.2146701.

Han, B., X., Yu, and E., Kwon. 2009. A self-sensing carbon nanotube/cement composite for traffic monitoring. *Nanotechnology*, 20(44): 445501. doi:10.1088/0957-4484/20/44/445501.

Hasegawa, T., Y. Kondo, Y. Koizumi, T. Sugiyama, A. Takeda, and S. Ito. 2009. A highly sensitive probe detecting low pH area of HeLa cells based on rhodamine B modified b-cyclodextrins. *Bioorganic & Medicinal Chemistry* 17:6015–9. doi:10.1016/j.bmc.2009.06.046.

Hayeeye, F., M. Sattar, W. Chinpa, and O. Sirichote. 2017. Kinetics and thermodynamics of rhodamine B adsorption by gelatin/activated carbon composite beads. *Colloids and Surfaces A: Physicochemical and Engineering Aspects*. 513:259–266. doi:10.1016/j.colsurfa.2016.10.052.

Hema, M., and S. Arivoli. 2009. Rhodamine B adsorption by activated carbon: kinetic and equilibrium studies. *Indian Journal of Chemical Technology* 16:38–45.

Hu, Z. Q., M., Li, M. D. Liu, W. M. Zhuang, and G. K. Li. 2013. A highly sensitive fluorescent acidic pH probe based on rhodamine B diethyl-2-aminobutenedioate conjugate and its application in living cells. *Dyes and Pigments* 96 (1):71–75. doi:10.1016/j.dyepig.2012.07.012.

Ibrahim, W. A. W., H. R., Nodeh, H. Y., Abul-Enein, and M. Sanagi. 2015. Magnetic solid-phase extraction based on modified ferum oxides for enrichment, preconcentration, and isolation of pesticides and selected pollutants. *Critical Reviews in Analytical Chemistry* 45:270–287. doi:10.1080/10408347.2014.938148.

Jain, R., M. Mathur, S. Sikarwar, and A. Mittal. 2007. Removal of the hazardous dye rhodamine B through photocatalytic and adsorption treatments. *Journal of Environmental Management* 85 (4): 956–964. doi:10.1016/j.jenvman.2006.11.002.

Jannah, N. R., and D. Onggo, 2019. Synthesis of Fe_3O_4 nanoparticles for colour removal of printing ink solution. *Journal of Physics: Conference Series* (1):1245. doi:10.1088/1742-6596/1245/1/012040.

Jiang, S., Li, Z., Yang, X., Li, M., Wang, C., Wang, Z., Wu, Q. 2023. Sustainable and green synthesis of porous organic polymer for solid-phase extraction of four chlorophenols in water and honey. *Food Chemistry* 404: 134652. doi:10.1016/j.foodchem.2022.134652.

Kennedy, J. F. Fang, J. Futter, J. Leveneur, P. P. Murmu, G. N. Panin, T. W. Kang, and E. Manikandan. 2017. Synthesis and enhanced field emission of zinc oxide incorporated carbon nanotubes. *Diamond and Related Materials* 71:79–84. doi:10.1016/j.diamond.2016.12.007.

Khan, T. A., S. Dahiya, and I. Ali. 2012. Use of kaolinite as adsorbent: Equilibrium, dynamics and thermodynamic studies on the adsorption of Rhodamine B from aqueous solution. *Applied Clay Science* 69:58–66. doi:10.1016/j.clay.2012.09.001.

Kim, H. N., M. H. Lee, H. J. Kim, J. S. Kim and J. Yoon. 2008. A new trend in rhodamine-based chemosensors: application of spirolactam ring-opening to sensing ions. *Chemical Society Reviews* 37:1465–1472. doi:10.1039/B802497A.

Kotsmar, E. V. C., V. B. Aksenenkob, V. Fainermanc, J. Pradinesa and R. Krägela. 2010. Miller. Equilibrium and dynamics of adsorption of mixed-casein/surfactant solutions at the water/hexane interface. *Colloids and Surfaces A: Physicochemical and Engineering Aspects* 354 (1–3): 210–217. doi:10.1016/j.colsurfa.2009.04.025.

Kumar, R., E. Joanni, R. K. Singh, P. Dinesh, and S. A., Moshkalev. 2015. Recent advances in the synthesis and modification of carbon-based 2D materials for application in energy conversion and storage. *Progress in Energy and Combustion Science* 67:115–157. doi:10.1016/j.pecs.2018.03.001.

Lee, J., S., Mahendra, and P. J. Alvarez. 2010. Nanomaterials in the construction industry: A review of their applications and environmental health and safety considerations. *ACS Nano*, 4(7): 3580–3590. doi:10.1021/nn100866w.

Li, C., H. Duan, X. Wang, X. Meng, and D. Qin. 2015. Fabrication of porous resins via solubility differences for adsorption of cadmium (II). *Chemical Engineering Journal* 262:250–259. doi:10.1016/j.cej.2014.09.105.

Li, J., B., Zhao, L., Hao, W., Liu, C., Wang, Z., Wang, and Q., Wu. 2023. Preparation of magnetic hyper-crosslinked polymer for high efficient preconcentration of four aflatoxins in rice and sorghum samples. *Food Chemistry* 404:134688. doi:10.1016/j.foodchem.2022.134688.

Li, Z., S. Wu, J. Han, and S. Han. 2011. Imaging of intracellular acidic compartments with a sensitive rhodamine based fluorogenic pH sensor. *Analyst* 136:3698–3706. doi:10.1039/C1AN15108H.

Ma, C., X., Guo, T., Li, X., Jiang, L., Wang, B., Zhao, and Z., Zhang. 2023. Anion exchange resin/quartz sand bi-layer composite dynamic membranes in ultrafiltration for algae-laden water treatment. *Process Safety and Environmental Protection*, 176. doi:10.1016/j.psep.2023.06.087.

Ma, P. C., N. A., Siddiqui, G., Marom, and J. K. Kim. 2010. Dispersion and functionalization of carbon nanotubes for polymer-based nanocomposites: A review. *Composites Part A: Applied Science and Manufacturing* 41(10):1345–1367. doi:10.1016/j.compositesa.2010.07.003.

Namasivayam, C., Muniasamy, N., Gayatri, K., Rani, M., and Ranganathan, K. 2019. Removal of dyes from aqueous solutions by cellulosic waste orange peel. *Bioresource Technology*, 57:37–43. doi:10.1016/0960-8524(96)00044-2.

Nekoeinia M., M. K Dehkordi M. Kolahdoozan, and S. Yousefinejad. 2015. Preparation of epoxidized soybean oil-grafted Fe_3O_4–SiO_2 as a water-dispersible hydrophobic nanocomposite for solid-phase extraction of rhodamine B. *Microchemical Journal*, 129:236–242. doi:10.1016/j.microc.2016.07.001.

Nodeh, H. R., W. A. Wan Ibrahim, I. Ali, and M. M., Sanagi. 2016. Development of magnetic graphene oxide adsorbent for the removal and preconcentration of As (III) and As (V) species from environmental water samples. *Environmental Science and Pollution Research* 23:9759–9773. doi:10.1007/s11356-016-6137-z.

Ozkantar, N., M., Soylak, and M. Tuzen. 2017. Spectrophotometric detection of rhodamine B in tap water, lipstick, rouge, and nail polish samples after supramolecular solvent microextraction. *Turkish Journal of Chemistry* 41:987–994. doi:10.3906/kim-1702-72.

Rais, A., and K. Rajeev. 2010. Adsorption of amaranth dye onto alumina reinforced polystyrene. *Clean—Soil Air Water* 39 (1):74–82. doi:10.1002/clen.201000125.

Ramoraswi, N. O., and P. G. Ndungu. 2015. Photo-catalytic properties of TiO_2 supported on MWCNTs, SBA-15 and silica-coated MWCNTs nanocomposites. *Nanoscale Research Letters* 10: 427. doi:10.1186/s11671-015-1137-3.

Ramuthai, S., V. Nandhakumar, M. Thiruchelvi, S. Arivoli, and V. Vijayakumaran. 2009. Rhodamine B adsorption kinetic, mechanistic and thermodynamic studies. *Journal of Chemistry* 6 (1):363–S373. doi:10.1155/2009/470704.

Richardson, S. D., C. S. Wilson and K. A. Rusch. 2004. Use of rhodamine water tracer in the marshland upwelling system. *Ground Water*. 42 (5):678–688. doi:10.1111/j.1745-6584.2004.tb02722.x.

Ruthven. D. M. 1984. *Principles of adsorption, desorption processes*. New York: Wiley.

Schieder, D., B. Dobias, E. Klumpp, and M. J. Schwuger. 1994. Adsorption and solubilisation of phenols in the hexadecyltrimethylammonium chloride adsorbed layer on quartz and corundum. *Colloids and Surfaces A: Physicochemical and Engineering Aspects* 88 (1):103–111. doi:10.1016/0927-7757(94)80090-1.

Shimada, T., H. Yamazaki, M. Mimura, Y. Inui, and Guengerich, F. P. 1994. Interindividual variations in human liver cytochrome P-450 enzymes involved in the oxidation of drugs, carcinogens, toxic chemicals: studies with liver microsomes of 30 Japanese, 30 Caucasians. *Journal of Pharmacology and Experimental Therapy*, 270:414–423.

Sldozian, R. J., Z., Mikhaleva, and A., Tkachev. 2019. Evaluation of the efficiency of lightweight concrete modified with additives based on nanostructures. *IOP Conference Series: Materials Science and Engineering* 693 (1): 012009. doi:10.1088/1757-899X/693/1/012009.

Sotouneh, F., M. R. Jamali, A. Asghari, M. Rajabi, 2023. Simultaneous preconcentration and determination of trace metals in edible plants and water samples by a novel solvent bar microextraction using a meltblown layer of facemask as the extractant phase holder combined with FAAS. *Microchemical Journal* 190: 108622, doi:10.1016/j.microc.2023.108622.

Soylak, M., L. Elci, and M. Dogan, 1997. Determination of trace amounts of cobalt in natural water samples as 4-(2-thiazolylazo) recorcinol complex after adsorptive preconcentration. *Analytical Letters* 30: 623–631. doi:10.1080/00032719708001806.

Soylak, M., Acar, D., Yilmaz, E., El-Khodary, S. A., Morsy, M., and Ibrahim, M. 2017. Magnetic graphene oxide as an efficient adsorbent for the separation and preconcentration of Cu (II), Pb (II), and Cd (II) from environmental samples. *Journal of AOAC International*, 100(5): 1544–1550. doi:10.5740/jaoacint.16-0230.

Soylak, M., and R., Maulana. 2023. Ultrasound assisted magnetic solid phase extraction of copper(II) and lead(II) in environmental samples on magnetic activated carbon cloth. *International Journal of Environmental Analytical Chemistry* 103(11): 2542–2554. doi:10.1080/03067319.2021.1895136.

Soylak, M., and Yilmaz, E. 2010. Sorbent extraction of 4-(2-thiazolylazo) resorcinol (TAR)–metal chelates on Diaion SP-850 adsorption resin in order to preconcentration/separation. *Journal of Hazardous Materials*, 182(1–3): 704–709. doi:10.1016/j.jhazmat.2010.06.089.

Soylak, M. 1998. Determination of trace amounts of copper in high-purity aluminum samples after preconcentration on an activated carbon column. *Fresenius Environmental Bulletin* 7: 383–387.

Su, X., X. Li, J. Li, M. Liu, F. Lei, X. Tan, P. Li, and W. Luo. 2015. Synthesis and characterization of core–shell magnetic molecularly imprinted polymers for solid-phase extraction and determination of Rhodamine B in food. *Food Chemistry* 171:292–297 doi:10.1016/j.foodchem.2014.09.024.

Sun, M., J. Wang, X. Mingsheng, Z. Fang, L. Jiang, Q. Han, J. Liu, M. Yan, Q. Wang, and H. Bi. 2019. Hybrid supercapacitors based on interwoven CoO-NiO-ZnO nanowires and porous graphene hydrogel electrodes with safe aqueous electrolyte for high supercapacitance. *Advance Electronic Materials* 5 (12):1900397. doi:10.1002/aelm.201900397.

Suzuki, M., ed. 1993. *Fundamentals of adsorption IV*. Tokyo: Kodansha.

Taziki, M., F. Shemirani, and B. Majidi. 2012. Robust ionic liquid against high concentration of salt for preconcentration and determination of rhodamine B. *Separation and Purification Technology* 97:216–220. doi:10.1016/j.seppur.2012.02.029.

Tercan, M., O. Dayan, and N. Özdemir, 2023. Simultaneous reduction of 4-nitrophenol, 4-nitroaniline and methylene blue organic pollutants via TiO_2 supported Pd(II) complex catalyst

bearing 2-(6-methylpyridin-2-yl)-1H-benzimidazole type ligand. *Polyhedron*, 232: 116297, doi: 10.1016/j.poly.2023.116297.

Tourchi Moghadam, M., and M., Seifi. 2022. Fabrication and investigation of ZnO-CNT@Fe_3O_4/NF as supercapacitor electrode by using a novel preparation method of CNT. *Diamond & Related Materials* 125:108962. doi:10.1016/j.diamond.2022.108962.

Wang, J., S., Dong, S., Dai Pang, C., Zhou, and B., Han. 2022. Pore structure characteristics of concrete composites with surface-modified carbon nanotubes. *Cement and Concrete Composites*, 128: 104453. doi:10.1016/j.cemconcomp.2022.104453.

Wang, Q., S., Zhang, Z., Li, Z., Wang, C., Wang, S., Alshehri, Y., Bando, Y., Yamauchi, and Q., Wu. 2023. Design of hyper-cross-linked polymers with tunable polarity for effective preconcentration of aflatoxins in grain. *Chemical Engineering Journal* 453: 139544. doi:10.1016/j.cej.2022.139544.

Wang, Y., Y. Mu, Q.B. Zhao, H., and Q. Yu. 2006. Isotherms, kinetics and thermodynamics of dye biosorption by anaerobic sludge. *Separation and Purification Technology* 50:1–7. doi:10.1016/j.seppur.2005.10.012.

Wu, Q., Y., Song, Q., Wang, W., Liu, L., Hao, Z., Wang, and C., Wang. 2022. Combination of magnetic solid-phase extraction and HPLC-UV for simultaneous determination of four phthalate esters in plastic bottled juice. *Food Chemistry* 339: 127855. doi:10.1016/j.foodchem.2020.127855.

Wu, Z. L., Q. Liu, X. O. Chen, and J. G. Yu. 2015. Preconcentration and analysis of Rhodamine B in water and red wine samples by using magnesium hydroxide/carbon nanotube composites as a solid-phase extractant. *Journal of Separation Science* 38:3404–3411. doi:10.1002/jssc.201500246.

Xolani, G., E. A. A. Mbuyise, K. Arbab, G. Kaviyarasu, M. Pellicane, and G. T. M. Maaza. 2017. Zinc oxide doped single wall carbon nanotubes in hole transport buffer layer. *Journal of Alloys and Compounds* 706: 344–350. doi:10.1016/j.jallcom.2017.02.249.

Xu, M., J., Wang, L., Zhang, Q., Wang, W., Liu, Y., An, L., Hao, C., Wang, Z., Wang, and Q., Wu. 2022. Construction of hydrophilic hypercrosslinked polymer based on natural kaempferol for highly effective extraction of 5-nitroimidazoles in environmental water, honey and fish samples. *Journal of Hazardous Materials* 429: 128288. doi:10.1016/j.jhazmat.2022.128288.

Xu, M., Z., Zhou, L., Hao, Z., Li, J., Li, Q., Wang, W., Liu, C., Wang, Z., Wang, and Q., Wu. 2023. Phenyl-imidazole based and nitrogen rich hyper-crosslinked polymer for sensitive determination of aflatoxins. *Food Chemistry* 405:134847. doi:10.1016/j.foodchem.2022.134847.

Yadollah, Y., F. Mohammad, and A. Mahnaz. 2015. Magnetic silica nanomaterials for solid-phase extraction combined with dispersive liquid-liquid microextraction of ultra-trace quantities of plasticizers. *Microchimica Acta* 182:1491–1499. doi:10.1007/s00604-015-1474-z.

Yang, L., J. Yang, X. Liu, Y. Zhang, Y. Wang, H. Fan, D. Wang, and J. Lang. 2008. Low-temperature synthesis and characterization of ZnO quantum dots. *Journal of Alloys and Compounds*. 463:92–95. doi:10.1016/j.jallcom.2007.12.006.

Yang, Z. F., L. Y. Li, L. C. Te-Hsieh, and R. S., Juang. 2018. Co-precipitation of magnetic Fe_3O_4 nanoparticles onto carbon nanotubes for removal of copper ions from aqueous solution. *Journal of the Taiwan Institute of Chemical Engineers* 82:56–63. doi:10.1016/j.jtice.2017.11.009.

Yuan, L., W. Lin, and Y. Feng. 2011. A rational approach to tuning the pKa values of rhodamines for living cell fluorescence imaging. *Organic & Biomolecular Chemistry* 9:1723–1726. doi:10.1039/C0OB01045F.

Zhang, H., and H. Selim. 2005. Kinetics of arsenate adsorption–desorption in soils. *Environmental Science & Technology* 39:6101–6108. doi:10.1021/es050334u.

Zhang, P., J. Su, J., Guo, and S., Hu. 2023. Influence of carbon nanotube on properties of concrete: A review. *Construction and Building Materials* 369: 130388. doi:10.1016/j.conbuildmat.2023.130388.

Zhang, W., B. Tang, Y. Liu, K. Xu, Y. Liu, and K. Xu. 2009. A highly sensitive acidic pH fluorescent probe and its application to HepG2 cells. *Analyst* 134:367–371. doi:10.1039/B807581F.

Zhou, W., W. Zhang, and Y. Cai. 2022. Enzyme-enhanced adsorption of laccase immobilized graphene oxide for micro-pollutant removal. *Separation and Purification Technology* 294:121178. doi:10.1016/j.seppur.2022.121178.